

The effect of metal oxide additives (WO_3 , MoO_3 , V_2O_5 , Ga_2O_3) on the oxidation of NO and SO_2 over Pt/ Al_2O_3 and Pt/ $\text{BaO}/\text{Al}_2\text{O}_3$ catalysts

Jazaer Dawody^{a,b,*}, Magnus Skoglundh^{a,c}, Erik Fridell^{a,b}

^a Competence Centre for Catalysis, Chalmers University of Technology, SE-41296 Göteborg, Sweden

^b Department of Applied Physics, Chalmers University of Technology, SE-41296 Göteborg, Sweden

^c Surface Chemistry, Chalmers University of Technology, SE-41296 Göteborg, Sweden

Received 12 July 2003; accepted 28 August 2003

Abstract

For NO_x storage, the oxidation of NO to NO_2 is an important step in the storage mechanism. In the first part of this work, model $\text{WO}_3/\text{Pt}/\text{Al}_2\text{O}_3$, $\text{MoO}_3/\text{Pt}/\text{Al}_2\text{O}_3$, $\text{V}_2\text{O}_5/\text{Pt}/\text{Al}_2\text{O}_3$, $\text{Ga}_2\text{O}_3/\text{Pt}/\text{Al}_2\text{O}_3$ and $\text{Pt}/\text{Al}_2\text{O}_3$ catalysts were prepared and used in flow reactor experiments. Heating ramp oxidation and steady state oxidation experiments were performed in order to investigate the catalytic activity for NO oxidation both in the presence and absence of SO_2 in the reaction gas mixture.

In the absence of SO_2 , the WO_3 and MoO_3 containing catalysts showed a significantly higher NO oxidation activity than the other catalysts. When SO_2 was included in the reaction gas mixture, the NO oxidation activity decreased for all catalysts, but the MoO_3 containing catalyst was less affected by the presence of SO_2 and also showed the lowest SO_2 oxidation activity.

In the second part of this work, model Pt/ $\text{BaO}/\text{Al}_2\text{O}_3$ and Pt/ $\text{BaO}/\text{MoO}_3/\text{Al}_2\text{O}_3$ catalysts were prepared and used in heating ramp oxidation and transient flow reactor experiments in order to investigate the effects of NO oxidation activity enhancement and suppression of the activity for SO_2 oxidation on NO_x storage capacity. Both catalysts showed equal NO_x storage capacity in the sulphur free cycles. When SO_2 was included in the reaction gas mixture, the NO_x storage capacity declined faster for the Pt/ $\text{BaO}/\text{MoO}_3/\text{Al}_2\text{O}_3$ catalyst than for the Pt/ $\text{BaO}/\text{Al}_2\text{O}_3$ catalyst, due to sulphur poisoning which resulted in a faster decrease in the regeneration capacity during rich periods.

© 2003 Elsevier B.V. All rights reserved.

Keywords: NO_x storage catalysts; Sulphur poisoning; NO oxidation; SO_2 oxidation; Metal oxide additives

1. Introduction

Vehicle combustion engines contribute significantly to the anthropogenic emissions of CO_2 . The increasing awareness of climate changes and the connection between accumulated CO_2 in the atmosphere and global warming [1,2] emphasises the need to reduce the vehicle fuel consumption. Diesel and lean burn engines have in this connection become important alternatives to the conventional gasoline engine, which operates close to stoichiometric air-to-fuel ratios. The main advantage with lean operation is the relatively low fuel consumption which can be 20–30% lower compared to stoichiometric combustion [3]. The exhausts from diesel and lean burn engines contain however, a large surplus of oxygen which prevents effective reduction of

nitrogen oxides (NO_x). To overcome this problem different techniques have been developed. One technique is selective catalytic reduction using ammonia as a reducing agent (NH_3 -SCR). Although the NO_x reduction potential of this technique is high, it has not yet been established in the market. The major obstacles are connected with the delivery systems of the reducing agents and the necessity of having a separate tank with ammonia or urea in the vehicle.

Another concept is to use NO_x storage catalysts, which function with alternating lean and rich conditions. During lean conditions NO is oxidised to NO_2 and trapped in a specific NO_x storage compound until the catalyst becomes saturated. To regenerate the catalyst, the conditions are switched during a short period (seconds) to rich conditions where the stored nitrates are released and decomposed to NO_2 and NO, and reduced to N_2 [4–6].

One major problem with the NO_x storage catalyst is its sensitivity to sulphur poisoning where sulphur compounds

* Corresponding author. Tel.: +46-31-7723153; fax: +46-31-7723134.
E-mail address: jazaer.dawody@fy.chalmers.se (J. Dawody).

are converted in the catalyst and trapped as sulphates with the NO_x storage compound [7]. Sulphate formation originates from the undesired SO_2 oxidation, which takes place simultaneously with NO oxidation during lean conditions. Since sulphates are thermally more stable than nitrates, the amount as well as the size of stored sulphate particles increase with increasing sulphur exposure time resulting in deactivation of the NO_x storage function [7].

Several studies have been performed with the aim of understanding, avoiding or at least suppressing the sulphur poisoning in NO_x storage catalysts. The outcome of these studies shows that parameters such as regeneration gas composition, lean-to-rich time ratio, temperature, choice of the storage material, as well as the noble metal(s) and the acidity of the support material play an important role both for the storage of NO_x and the poisoning by sulphur [8–16].

During recent years different ways to minimise sulphur poisoning of NO_x storage catalysts have been suggested. In some of these studies, sulphate decomposition and SO_x desorption were enhanced by catalyst washcoat modification with components such as TiO_2 , Rh/ZrO₂, Fe and Li in order to prevent the growth of sulphate particles and/or stimulate hydrogen generation for enhancing the reduction of barium sulphates [17–20].

It has also been shown that interaction between sulphur and the noble metal particles during rich conditions is of significant importance for the deactivation [13,16,21].

Formation of sulphates may also be suppressed by designing the catalyst so that the NO_2 formation is enhanced in relation to SO_2 oxidation, which is an important step for NO_x storage. It might be possible to suppress the oxidation of SO_2 to SO_3 by changing the structure of the active catalyst particles, since this reaction seems to be structure sensitive [22]. Another way may be to add additives which inhibit or at least suppress the oxidation of SO_2 .

Transition metal oxides such as V_2O_5 , MoO_3 and WO_3 are widely used in NH_3 -SCR catalysts due to their redox properties, which seem to be important in enhancing NO conversion. In addition, they contribute to increasing the surface acidity [23–27] which might suppress the SO_2 oxidation.

Ga_2O_3 has been used in selective catalytic reduction of NO_x with hydrocarbons (HC-SCR) [28–33]. For a Ga_2O_3 - Al_2O_3 catalyst, two types of Lewis acid sites were defined [33]. According to Pasel et al. [28], the presence of SO_2 in the gas feed did not strongly affect the catalytic activity in NO conversion for a Ga_2O_3 loaded sulphated zirconia catalyst.

The aim of this study is to investigate if a set of metal oxides can act as promoters to enhance the NO oxidation and/or suppress the SO_2 oxidation. In the first part of the study, alumina supported Pt catalysts with and without metal oxide additives were prepared and the catalytic activity of both separate and simultaneous NO and SO_2 oxidation were investigated. In the second part of the study, one unmodified and one MoO_3 modified NO_x storage catalyst were prepared

with BaO as storage component and the NO_x storage capacity was investigated by performing lean/rich transient flow reactor experiments.

2. Experimental

2.1. Catalyst preparation

Seven cordierite monoliths (400 cells/in.²) with a length of 15 mm containing 188 channels were washcoated with alumina and five of the samples were impregnated with platinum. Four of the platinum containing samples were also provided with either, MoO_3 , WO_3 , V_2O_5 or Ga_2O_3 . Finally, one of the remaining two alumina coated samples was provided with V_2O_5 and the other with MoO_3 .

The catalysts were prepared according to the method described in detail in [34]. Briefly, the monoliths were impregnated with alumina by immersing the monolith in an alumina slurry, blowing away the excess of the slurry from the channels, drying in air at 95 °C for few seconds and calcining in air at 500 °C for 2 min. This procedure was repeated until the desired amount of alumina was obtained. Thereafter, the samples were calcined at 500 °C for 2 h. The desired amount of Pt was added to the alumina coated samples by filling the channels with an aqueous solution of platinum nitrate [$\text{Pt}(\text{NO}_3)_2$] and drying at 90 °C for 12 h, and then calcining in air at 500 °C for 2 h. To provide the metal oxide additives, each alumina and Pt coated monolith was impregnated with one of the following additive aqueous solutions: ammonium molybdate [$(\text{NH}_4)_2\text{Mo}_2\text{O}_7$], ammonium tungsten oxide [$(\text{NH}_4)_{10}\text{W}_{12}\text{O}_{41}\cdot x\text{H}_2\text{O}$], gallium nitrate [$\text{Ga}(\text{NO}_3)_3$] or vanadium oxalate [$\text{VO}(\text{C}_2\text{O}_4)^{2-}$]. After the impregnation with the additive precursor solutions, the samples were dried and finally calcined in air at 500 °C for 2 h.

For the NO_x storage experiments, one Pt/BaO/ Al_2O_3 and one Pt/BaO/ MoO_3 / Al_2O_3 catalyst were prepared. The size of these catalysts as well as the washcoat impregnation method was the same as for the catalysts described above. The Pt/BaO/ Al_2O_3 catalyst was prepared by impregnation with alumina, followed by impregnation with an aqueous barium nitrate [$\text{Ba}(\text{NO}_3)_2$] solution and finally Pt precursor solution. For the Pt/BaO/ MoO_3 / Al_2O_3 catalyst, the impregnation with molybdate solution was performed before the impregnation with BaO in order to avoid BaO dissolving since the molybdate solution is slightly acidic and to ensure that equal amount BaO in both catalysts are accessible for barium nitrate formation. Further, in order to avoid BaO dissolving when impregnating with the acidic platinum nitrate solution, the catalysts were immersed in a solution of ammonium carbamate ($\text{NH}_4\text{CO}_2\text{NH}_2$) and the excess solution was removed from the channels by air immediately before impregnation with the Pt precursor solution.

The compositions of the washcoat materials for all catalysts prepared are given in Table 1.

Table 1
Catalyst washcoat compositions

Samples	Al ₂ O ₃ (mg)	Pt (mg)	Metal additive (mmol)	BaO-content (mg)
Pt/Al ₂ O ₃	623	13	–	–
MoO ₃ /Pt/Al ₂ O ₃	585	12	0.35	–
WO ₃ /Pt/Al ₂ O ₃	545	13	0.39	–
V ₂ O ₅ /Pt/Al ₂ O ₃	622	13	0.18	–
Ga ₂ O ₃ /Pt/Al ₂ O ₃	569	12	0.18	–
V ₂ O ₅ /Al ₂ O ₃	607	–	0.18	–
MoO ₃ /Al ₂ O ₃	574	–	0.35	–
Pt/BaO/MoO ₃ /Al ₂ O ₃	469	12	0.47	125
Pt/BaO/Al ₂ O ₃	490	13	–	125

2.2. Catalyst characterisation

The platinum dispersion of the platinum containing catalysts and the CO adsorption capacity of the MoO₃/Al₂O₃ and V₂O₅/Al₂O₃ samples were determined by temperature programmed desorption (TPD) of CO. The TPD experiments were conducted in a flow reactor with a quartz tube in which the catalyst was placed. A thermocouple used to control the temperature was placed a few mm in front of the catalyst. Another thermocouple was placed inside the catalyst to measure the catalyst temperature. A mass spectrometer (Balzer QME 120) was connected to the reactor to analyse the outflow gas composition. The gas flow into the reactor was controlled with mass flow controllers.

Prior to each measurement, the catalyst was first pre-oxidised and then pre-reduced at 500 °C with 2% O₂ in Ar and 4% H₂ in Ar, respectively. CO was adsorbed on the catalyst surface by exposing the catalyst to 2000 ppm CO in Ar at 4 °C for 10 min. The sample was then heated with a speed of 40 °C/min up to 550 °C in Ar and the desorbed species were analysed by the MS. The Pt dispersion was calculated by assuming an adsorption of 0.7 CO molecules per Pt surface atom [35].

The specific surface areas of the catalysts were determined by nitrogen adsorption according to the BET method using Digisorb 2600 (Micromeritics) instrument.

The platinum dispersion and the specific surface areas of the catalysts are given in Table 2.

2.3. Activity studies

The activity of the catalysts was tested in another flow reactor similar to the previously described one, but with other instruments to analyse the outflow gas compositions. A chemiluminescence detector (CLD 700) was used to monitor NO_x (NO and NO₂), while SO₂, CO₂ and N₂O were measured by separate non-dispersive IR Maihak UNOR 610 instruments. The inlet gas composition was controlled by an Environics 2000 gas mixer. The gas flow and space velocity in all experiments were 3000 ml/min and 38 000 h⁻¹, respectively, with Ar as the carrier gas.

Prior to each temperature ramp and steady state experiment the catalysts were pre-treated at 500 °C, first by reduction in 2% H₂ for 20 min, flushing with Ar for 5 min and finally oxidation in 8% O₂ for 20 min. After each pre-treatment, the catalyst was cooled down to room temperature in Ar. The gas compositions for all oxidation experiments are given in Table 3.

2.3.1. Heating ramp experiments

Each experiment started at room temperature by exposing the pre-treated catalyst to the reaction gas mixture until saturation (i.e. the outlet concentration of NO_x and/or SO₂ was equal to the inlet concentration), thereafter, the temperature was linearly increased by 5 °C/min to 450 °C in the same reaction gas mixture. The experiments were performed both with separate and simultaneous NO and SO₂ oxidations.

Table 2
Catalyst characterisation data

Samples	BET surface area (m ² /g catalyst)	Pt dispersion (%) fresh catalyst	Desorbed CO (μmol) fresh catalyst	Pt dispersion (%) used catalyst	Desorbed CO (μmol) used catalyst
Pt/Al ₂ O ₃	33	9.6	6.2	3.4	2.2
MoO ₃ /Pt/Al ₂ O ₃	32	7.7 ^a	9.4	12.6 ^a	11.5
WO ₃ /Pt/Al ₂ O ₃	31	10.4	4.5	1.5	0.64
Ga ₂ O ₃ /Pt/Al ₂ O ₃	31	10.7	4.6	4.7	2.0
V ₂ O ₅ /Pt/Al ₂ O ₃	34	14.9 ^a	18.3	18.4 ^a	20
V ₂ O ₅ /Al ₂ O ₃	n.d.	–	12	–	n.d.
MoO ₃ /Al ₂ O ₃	n.d.	–	6.1	–	n.d.

^a The amount of CO adsorbed on Pt = the difference between the integrated amount of CO desorbed from MeO/Pt/Al₂O₃ and MeO/Al₂O₃ (MeO = V₂O₅ or MoO₃).

Table 3
Summary of gas compositions

Experiment	NO (vol. ppm)	SO ₂ (vol. ppm)	O ₂ (vol.%)	C ₃ H ₆ (vol.%)
NO heating ramp oxidation	450	–	8	–
SO ₂ heating ramp oxidation	–	30	8	–
NO + SO ₂ heating ramp oxidation	450	30	8	–
NO steady state oxidation	450	–	8	–
SO ₂ steady state oxidation	–	30	8	–
NO + SO ₂ steady state oxidation	450	30	8	–
NO _x storage reduction lean condition	400	10	8	650
NO _x storage reduction rich condition	400	10	–	650

2.3.2. Steady state experiments

Steady state experiments were performed by saturating the pre-treated catalyst with the reaction gas mixture at room temperature in the same way as in the heating ramp experiments. Thereafter, the activity for NO and SO₂ oxidation was measured at 125, 150, 175, 200, 225 °C for 20 min at each temperature.

2.3.3. Transient experiments

Prior to the transient experiments, the NO_x storage catalysts were pre-treated at 550 °C by reduction in 2% H₂ for 30 min and cooling down to 300 °C in Ar. Thereafter, the catalyst was stabilised in a lean gas mixture for 20 min and regenerated in rich gas mixture for 4 min. The lean gas mixture composition was 400 ppm NO, 8% O₂ and 650 ppm C₃H₆ in Ar with a flow of 3000 ml/min. For the rich gas composition, the oxygen supply was switched off, and compensated by Ar to maintain constant flow. Transient experiments with lean/rich cycles were conducted at 300 °C with 16 and 4 min long lean and rich periods, respectively. Four sulphur free lean/rich cycles were initially performed, thereafter 10 ppm SO₂ was included in both the lean and the rich gas mixtures during the remaining cycles.

3. Results

3.1. Heating ramp experiments

3.1.1. NO oxidation

The catalytic activity for NO oxidation was investigated in oxygen excess both in absence and presence of SO₂.

Fig. 1 shows the concentration of NO₂ as a function of temperature in the absence of SO₂. As is clear from the figure, all catalysts show very low NO oxidation activity for temperatures up to ~130 °C. After further temperature increase, NO₂ starts to form at ~140 and 165 °C for the WO₃ and MoO₃ containing catalysts, respectively. The activity for NO oxidation is further lower for the Ga₂O₃ containing catalyst followed by the Pt/Al₂O₃ and finally the V₂O₅ containing catalyst. In all cases the NO₂ concentration increases until it reaches a maximum, and then starts to decrease as

the temperature is increased. This decrease is due to the NO₂ concentration becoming limited by the thermodynamic equilibrium concentration. For the WO₃ and MoO₃ containing catalysts, the NO₂ concentrations maxima are reached at ~220 °C with 92 and 81% NO conversion, respectively. The maximum in NO₂ concentration for the other three catalysts is reached at 300–330 °C with maximum conversions of 78, 77 and 67% for the Ga₂O₃ containing, Pt/Al₂O₃ and V₂O₅ containing catalysts, respectively.

In order to investigate the influence of SO₂ on the NO oxidation activity, 30 ppm SO₂ was included in the above mentioned reaction gas mixture. The results from these experiments are shown in Fig. 2 which displays the outlet NO₂ concentration as a function of temperature. It is obvious that the NO oxidation activity for all catalysts decreases in by the presence of SO₂. The formation of NO₂ is shifted towards higher temperatures. The NO₂ formation rate is lower and the maximum in NO₂ formation is lower compared with the corresponding experiments in absence of SO₂. The results from these experiments show two interesting features: (i) the Pt/Al₂O₃ catalyst seem to be more affected by the presence of SO₂ than for all catalysts with metal oxide additives; and (ii) despite the presence of SO₂ the MoO₃ and WO₃ containing catalysts still show much higher NO oxidation activity than the other catalysts.

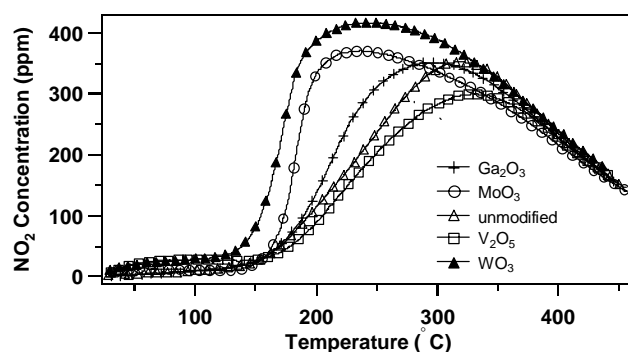


Fig. 1. NO₂ concentration as a function of temperature from separate NO oxidation experiments. Catalysts: MoO₃/Pt/Al₂O₃ (○); Ga₂O₃/Pt/Al₂O₃ (+); V₂O₅/Pt/Al₂O₃ (□); WO₃/Pt/Al₂O₃ (▲); Pt/Al₂O₃ (Δ). Temperature ramp = 5 °C/min. Gases: 450 vol. ppm NO and 8% O₂ in Ar. Total flow = 3000 ml/min.

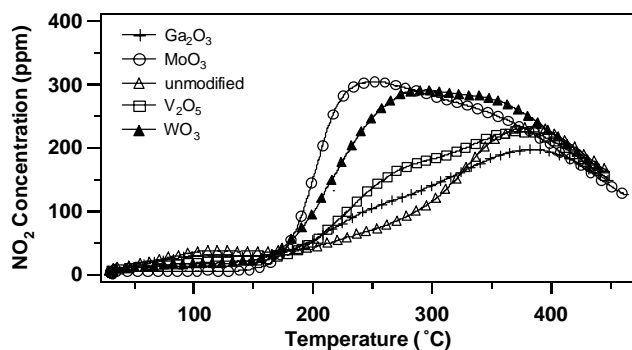


Fig. 2. NO_2 concentrations as a function of temperature from simultaneous NO and SO_2 oxidation experiments. Catalysts: $\text{MoO}_3/\text{Pt}/\text{Al}_2\text{O}_3$ (\circ); $\text{Ga}_2\text{O}_3/\text{Pt}/\text{Al}_2\text{O}_3$ (+); $\text{V}_2\text{O}_5/\text{Pt}/\text{Al}_2\text{O}_3$ (\square); $\text{WO}_3/\text{Pt}/\text{Al}_2\text{O}_3$ (\blacktriangle); $\text{Pt}/\text{Al}_2\text{O}_3$ (\triangle). Temperature ramp = $5^\circ\text{C}/\text{min}$. Gases: 450 vol. ppm NO, 30 ppm SO_2 and 8% O_2 in Ar. Total flow = 3000 ml/min.

3.1.2. SO_2 oxidation

In the same way as with NO oxidation, SO_2 heating ramp oxidation experiments were performed both in the absence and presence of NO in the reaction gas mixture. The results from the separate SO_2 oxidation experiments are shown in Fig. 3, while Fig. 4 displays the results for the SO_2 oxidation in the presence of NO. It is worth to point out that a decrease in the SO_2 concentration indicates SO_2 consumption, and since the experiments were performed with oxygen in excess, we believe that any decrease in the outlet SO_2 concentration is related to SO_2 adsorption and/or oxidation to SO_3 . Prior to each experiment, the pre-treated catalysts were saturated in the reaction gas mixture at room temperature until the outlet NO concentration was equal to the inlet concentration and the SO_2 concentration became very close to the inlet concentration (30 ppm). Table 4 displays the time which was required for detecting 20 ppm SO_2 in the outlet flow for all samples. As it is clear from the table, the Ga_2O_3 promoted catalyst followed by the $\text{Pt}/\text{Al}_2\text{O}_3$ catalyst adsorb much more SO_2 during the saturation step than the other catalysts. This may explain why the concentration of outlet SO_2 for these

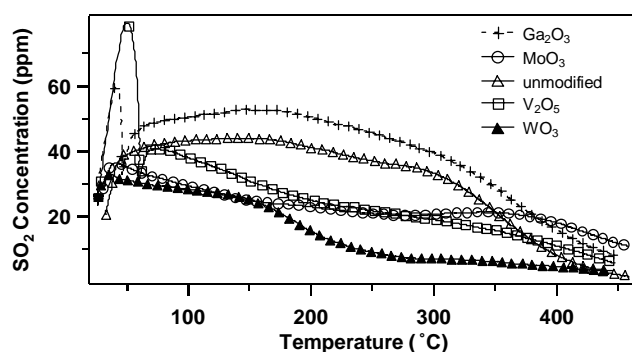


Fig. 3. SO_2 concentration as a function of temperature from separate SO_2 oxidation experiments. Catalysts: $\text{MoO}_3/\text{Pt}/\text{Al}_2\text{O}_3$ (\circ); $\text{Ga}_2\text{O}_3/\text{Pt}/\text{Al}_2\text{O}_3$ (+); $\text{V}_2\text{O}_5/\text{Pt}/\text{Al}_2\text{O}_3$ (\square); $\text{WO}_3/\text{Pt}/\text{Al}_2\text{O}_3$ (\blacktriangle); $\text{Pt}/\text{Al}_2\text{O}_3$ (\triangle). Temperature ramp = $5^\circ\text{C}/\text{min}$. Gases: 30 vol. ppm SO_2 and 8% O_2 in Ar. Total flow = 3000 ml/min.

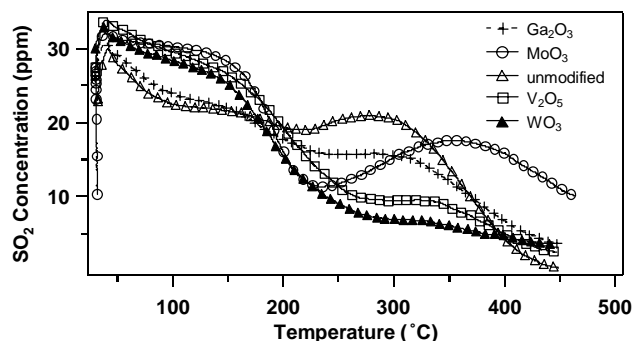


Fig. 4. SO_2 concentrations as a function of temperature from simultaneous NO and SO_2 oxidation experiments. Catalysts: $\text{MoO}_3/\text{Pt}/\text{Al}_2\text{O}_3$ (\circ); $\text{Ga}_2\text{O}_3/\text{Pt}/\text{Al}_2\text{O}_3$ (+); $\text{V}_2\text{O}_5/\text{Pt}/\text{Al}_2\text{O}_3$ (\square); $\text{WO}_3/\text{Pt}/\text{Al}_2\text{O}_3$ (\blacktriangle); $\text{Pt}/\text{Al}_2\text{O}_3$ (\triangle). Temperature ramp = $5^\circ\text{C}/\text{min}$. Gases: 450 vol. ppm NO, 30 vol. ppm SO_2 and 8% O_2 in Ar. Total flow = 3000 ml/min.

two catalysts in Fig. 3 is higher than the inlet SO_2 concentration at temperatures $<250^\circ\text{C}$. The peaks which appear at low temperatures in the beginning of the heating ramps can be related to desorption of weakly adsorbed SO_2 . Concerning the SO_2 oxidation activity, it is obvious that the WO_3 containing catalyst shows high SO_2 oxidation activity not only in the separate SO_2 oxidation experiments, but also in the simultaneous SO_2 and NO oxidation experiments (see Figs. 3 and 4). As can be seen in Table 4, the saturation time with SO_2 for the Ga_2O_3 containing catalyst and the unmodified catalyst in the experiment with simultaneous NO and SO_2 exposure is shorter compared to the corresponding saturation time in the separate SO_2 oxidation experiment. This is seen from the appearance of the temperature ramp curves in Fig. 4, where the low temperature desorption peaks almost disappear and the outlet SO_2 concentrations decline below the inlet concentration at the beginning of the temperature ramp. The lowest SO_2 oxidation activity both in the presence and in the absence of NO is shown by the MoO_3 containing catalyst.

3.2. Steady state experiments

3.2.1. NO oxidation

Figs. 5 and 6 show the outlet concentration of NO_2 as a function of time at 125, 150, 175, 200 and 225°C with a step of 20 min at each temperature in the absence and presence

Table 4

The time required for detecting 20 ppm SO_2 in the outlet flow during the saturation step performed on the catalysts prior to the heating ramp experiments both in the presence and absence of NO in the reaction gas mixture

NO	SO_2 saturation time with NO in the feed (min)	SO_2 saturation time without in the feed (min)
$\text{Pt}/\text{Al}_2\text{O}_3$	48	64
$\text{Ga}_2\text{O}_3/\text{Pt}/\text{Al}_2\text{O}_3$	52	93
$\text{WO}_3/\text{Pt}/\text{Al}_2\text{O}_3$	28	31
$\text{V}_2\text{O}_5/\text{Pt}/\text{Al}_2\text{O}_3$	21	18
$\text{MoO}_3/\text{Pt}/\text{Al}_2\text{O}_3$	8	7

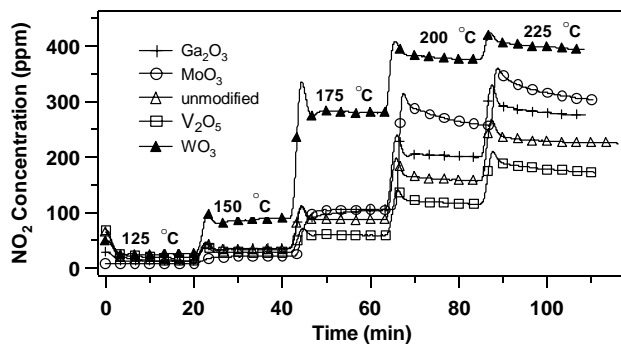


Fig. 5. NO₂ concentration as a function of time measured at the temperatures: 125, 150, 175, 200 and 225 °C. Catalysts: MoO₃/Pt/Al₂O₃ (O); Ga₂O₃/Pt/Al₂O₃ (+); V₂O₅/Pt/Al₂O₃ (□); WO₃/Pt/Al₂O₃ (▲); Pt/Al₂O₃ (Δ). The temperature between the steps was increased with 15 °C/min. Gases: 450 vol. ppm NO, 8% O₂ in Ar with a total flow of 3000 ml/min.

of SO₂, respectively. The highest NO oxidation activities in NO steady state oxidation experiments are shown by the WO₃ containing catalyst followed by the MoO₃/Pt/Al₂O₃ catalyst. The order in activity for the other three catalysts is: Ga₂O₃/Pt/Al₂O₃ > Pt/Al₂O₃ > V₂O₅/Pt/Al₂O₃. The addition of SO₂ to the gas mixture deteriorates the NO oxidation activity resulting in decreased outlet NO₂ concentration levels at all temperatures for all catalysts (see Fig. 6). The order in NO oxidation activity is still in agreement with the results from the simultaneous NO and SO₂ heating ramp experiments with the exception for the Pt/Al₂O₃ catalyst which shows higher NO₂ formation at 200 and 225 °C compared to the concentration levels at the same temperatures in the heating ramp oxidation experiment.

The results from NO steady state oxidation experiments conducted in the presence of SO₂ show that the MoO₃ containing catalyst and the WO₃/Pt/Al₂O₃ catalyst still show significantly higher NO oxidation activity than the other catalysts as they also do in the corresponding heating ramp oxidation experiments.

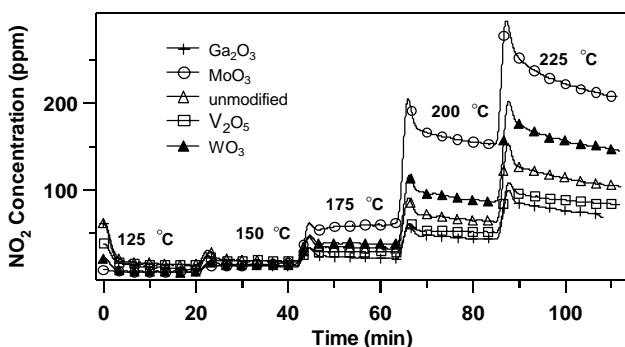


Fig. 6. NO₂ concentration as a function of time in the presence of SO₂ measured at the temperatures: 125, 150, 175, 200 and 225 °C. Catalysts: MoO₃/Pt/Al₂O₃ (O); Ga₂O₃/Pt/Al₂O₃ (+); V₂O₅/Pt/Al₂O₃ (□); WO₃/Pt/Al₂O₃ (▲); Pt/Al₂O₃ (Δ). The temperature between the steps was increased with 15 °C/min. Gases: 450 vol. ppm NO, 30 vol. ppm SO₂, 8% O₂ in Ar with a total flow of 3000 ml/min.

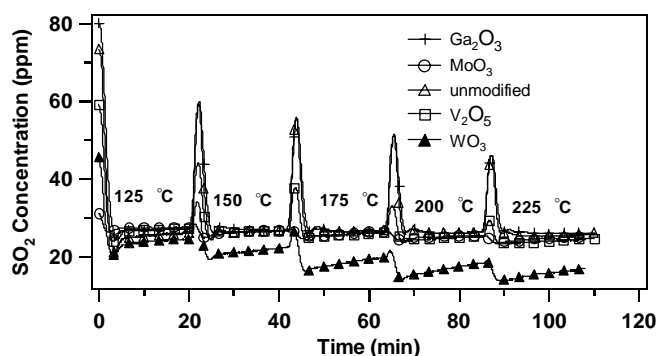


Fig. 7. SO₂ concentration as a function of time measured at the temperatures: 125, 150, 175, 200 and 225 °C. Catalysts: MoO₃/Pt/Al₂O₃ (O); Ga₂O₃/Pt/Al₂O₃ (+); V₂O₅/Pt/Al₂O₃ (□); WO₃/Pt/Al₂O₃ (▲); Pt/Al₂O₃ (Δ). The temperature between the steps was increased with 15 °C/min. Gases: 30 vol. ppm SO₂, 8% O₂ in Ar with a total flow of 3000 ml/min.

3.2.2. SO₂ oxidation

SO₂ steady state oxidation was performed in the absence and presence of NO in the same way as in NO steady state oxidation. The results from SO₂ oxidation experiments in the absence of NO are shown in Fig. 7. The SO₂ peaks which appear between the steady state steps are due to SO₂ desorption caused by the temperature increase. Even in the steady state experiments, higher amounts of SO₂ were adsorbed on the Ga₂O₃ containing and the Pt/Al₂O₃ catalysts, which give the high desorption SO₂ peaks when the temperature was increased between the steady state steps. As it is clear from the figure, the measured SO₂ concentrations at all temperatures for all catalysts are similar, except for the WO₃ containing catalyst which shows ~30% higher oxidation of SO₂ at these temperatures compared to the other catalysts. When NO is included in the reaction gas mixture (Fig. 8), the Pt/Al₂O₃ catalyst shows the highest SO₂ oxidation activity at all temperature steps.

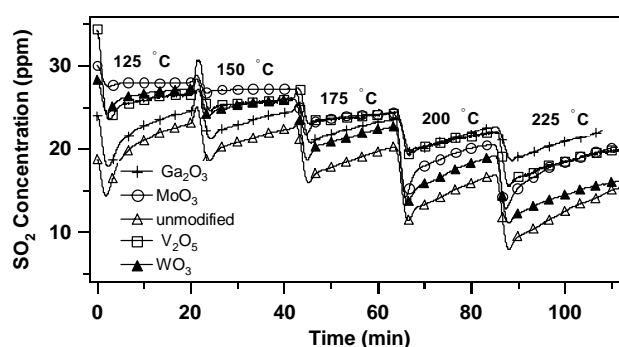


Fig. 8. SO₂ concentration as a function of time in the presence of NO measured at the temperatures: 125, 150, 175, 200 and 225 °C. Catalysts: MoO₃/Pt/Al₂O₃ (O); Ga₂O₃/Pt/Al₂O₃ (+); V₂O₅/Pt/Al₂O₃ (□); WO₃/Pt/Al₂O₃ (▲); Pt/Al₂O₃ (Δ). The temperature between the steps was increased with 15 °C/min. Gases: 450 vol. ppm NO, 30 vol. ppm SO₂, 8% O₂ in Ar with a total flow of 3000 ml/min.

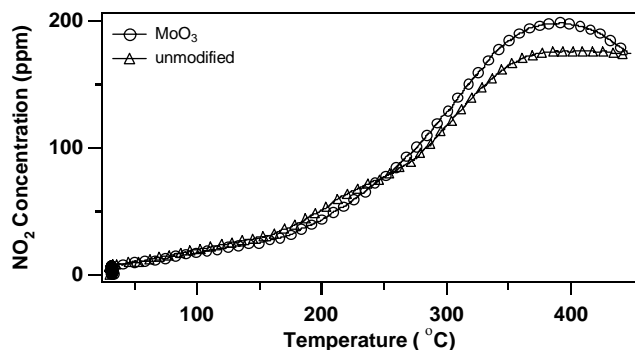


Fig. 9. NO₂ concentration as a function of temperature from heating ramp NO oxidation performed on Pt/BaO/MoO₃/Al₂O₃ (○) and Pt/BaO/Al₂O₃ (Δ) catalysts. Ramp rate = 5 °C/min. Gases: 450 ppm NO, 8% O₂ in Ar with a total flow of 3000 ml/min.

3.3. NO_x storage experiments

3.3.1. Heating ramp experiments

Heating ramp experiments with NO/O₂ mixture were conducted with model Pt/Ba/MoO₃/Al₂O₃ and Pt/BaO/Al₂O₃ catalysts using the same procedure and gas composition as in Section 3.1.1 and Table 3, respectively. As can be seen in Fig. 9, the NO oxidation activity for the Pt/BaO/MoO₃/Al₂O₃ catalyst is slightly higher than for the Pt/BaO/Al₂O₃ catalyst, but significantly lower than for the MoO₃/Pt/Al₂O₃ catalyst (see Fig. 1).

3.3.2. Transient NO_x storage experiments

The results from the transient experiments using the two barium containing catalysts are shown in Fig. 10. The continuous and broken lines denote NO_x and NO₂ outlet concentrations for the Pt/BaO/MoO₃/Al₂O₃ and Pt/BaO/Al₂O₃ catalysts, respectively. In the initial lean periods, the storage of NO_x is seen from the relatively slow increase of the NO_x signal up to a steady state level. During the rich period the outlet NO_x signal becomes lower as the incoming and stored NO_x is reduced. The amount of stored NO_x is calculated by

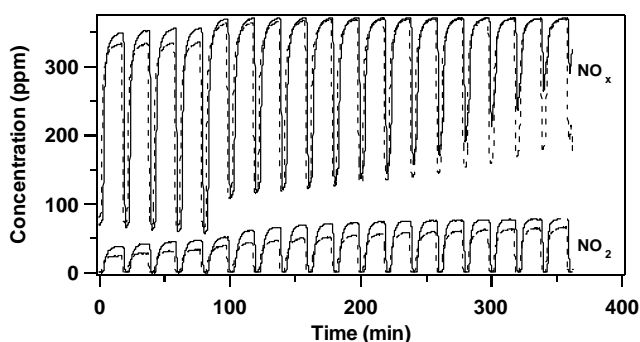


Fig. 10. Measured NO_x and NO₂ over a Pt/BaO/MoO₃/Al₂O₃ (continuous line) and a Pt/BaO/Al₂O₃ (broken line) catalyst during transient experiments. The composition of lean gas mixture was 400 ppm NO, 650 ppm C₃H₆, 8% O₂ and for rich condition, O₂ was switched off. 10 ppm SO₂ was added to lean and rich gas mixtures from the fifth cycle. The total gas flow was constant during the entire experiment time.

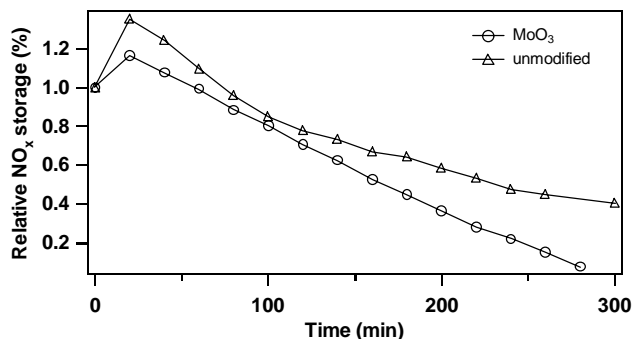


Fig. 11. Normalized NO_x storage capacity as a function of SO₂ exposure time for Pt/BaO/MoO₃/Al₂O₃ (○) and Pt/BaO/Al₂O₃ (Δ) catalysts.

subtracting the integrated amount of outlet NO_x from the integrated amount of inlet NO_x for each lean period.

Some interesting features in the NO_x storage experiments are: (1) the steady state NO_x levels for both catalysts immediately become higher when SO₂ is added to the gas mixture; (2) both catalysts have relatively high storage capacity in the sulphur free cycles; (3) the amount of unreduced NO_x during the rich periods is gradually increased with increased sulphur exposure time, especially for the MoO₃ containing catalyst.

In order to investigate the impact of sulphur exposure on the NO_x storage capacity and at the same time compare the catalysts with each other, a mean NO_x storage value was calculated from the four sulphur free cycles and the NO_x storage in the remaining cycles normalised to this value. The resulting NO_x storage as a function of time during SO₂ exposure is shown in Fig. 11. Obviously, the MoO₃ containing catalyst becomes deactivated by sulphur more quickly than the Pt/BaO/Al₂O₃ catalyst which is manifested in the faster decay of the NO_x storage capacity.

4. Discussion

4.1. NO oxidation

Our aim was to prepare catalysts with constant Pt-loading (0.062 mmol), constant amount additives (0.345 mmol) and constant amount of washcoat corresponding to 20 wt.% of the catalyst mass.

From the catalyst characterisation data in Table 2, it is clear that the specific surface area of the samples is almost constant, which means that the addition of metal oxide additives does not result in any significant decrease in surface area.

The Pt dispersion values which are displayed in Table 2 are obtained by taking into account that CO in addition to Pt, also can be adsorbed to the metal oxide additives. For this reason, temperature programmed CO desorption experiments were performed on alumina supported metal oxide samples without Pt. It was found that significant amounts of CO adsorb on V₂O₅ and MoO₃. Thus, the Pt dispersions

for the $\text{MoO}_3/\text{Pt}/\text{Al}_2\text{O}_3$ and $\text{V}_2\text{O}_5/\text{Pt}/\text{Al}_2\text{O}_3$ catalysts were calculated by subtracting the integrated amount of desorbed CO from the Pt-free samples from the corresponding amount CO for the Pt-containing samples. The Pt dispersion achieved using this method does not take into account for CO adsorbed on interfacial Pt–Me sites or spill over of the CO from Pt- to Me-sites, which may occur during the experiment. The Pt dispersions for the $\text{MoO}_3/\text{Pt}/\text{Al}_2\text{O}_3$ and $\text{V}_2\text{O}_5/\text{Pt}/\text{Al}_2\text{O}_3$ samples are therefore somewhat uncertain.

As it is seen from the Table, the Pt dispersions for the samples before performing the activity measurements are roughly in the same range. Further, the Pt dispersions for all samples except for the V_2O_5 and MoO_3 containing catalysts are significantly lowered after performing the activity measurements. The decrease in Pt dispersion may indicate increased Pt particle sizes, probably due to the exposure to sulphur [36].

The results from the temperature ramp and steady state oxidation of NO show that WO_3 and MoO_3 seem to be the most active additives in enhancing the activity for NO oxidation. As it is seen from Fig. 1, the addition of either of these two metal oxides results in higher NO oxidation activity where NO_2 forms with significantly higher rate and reaches higher outlet concentration values in comparison to the other catalysts. Obviously, WO_3 has the highest promoting effect on the NO oxidation activity in sulphur free atmosphere, since the NO_2 formation for the WO_3 containing catalyst starts at markedly lower temperature and reaches a higher conversion (92%) compared to the other catalysts. Fig. 1 shows another feature which is worth to mention, namely that the presence of V_2O_5 slightly suppresses the NO oxidation activity. What this depends on is not clear. It can be a consequence of the high Pt dispersion for this catalyst. According to Olsson and Fridell [37] alumina supported catalysts with smaller Pt particles show lower NO oxidation activity than catalysts with larger Pt particles since the probability for platinum oxide formation is higher on smaller Pt particles.

Concerning the effect of Ga_2O_3 on enhancing the NO oxidation, the results show that Ga_2O_3 slightly promotes this reaction in the absence of SO_2 .

The NO oxidation activity for all catalysts deteriorates when SO_2 is included in the reaction gas mixture (see Fig. 2). For each catalyst, the decrease in NO_2 formation due to SO_2 exposure can be obtained by subtracting the NO_2 outlet concentration curve obtained from the experiments with simultaneous SO_2 and NO exposure from the corresponding NO oxidation experiment. Such a calculation shows that the NO_2 formation decreases in the following order: $\text{Pt}/\text{Al}_2\text{O}_3 > \text{Ga}_2\text{O}_3/\text{Pt}/\text{Al}_2\text{O}_3 > \text{WO}_3/\text{Pt}/\text{Al}_2\text{O}_3 > \text{V}_2\text{O}_5/\text{Pt}/\text{Al}_2\text{O}_3 > \text{MoO}_3/\text{Pt}/\text{Al}_2\text{O}_3$. This means that the NO oxidation activity is most affected in the absence of metal oxide additives. Of the tested metal oxides, MoO_3 seems to be the most promising SO_2 oxidation inhibitor.

The results from the NO steady state oxidation experiments conducted in the absence of SO_2 and shown in Fig. 3 are in agreement with the results from the separate NO heat-

ing ramp experiments. The NO_2 outlet concentrations at all temperature steps for all samples can be considered as steady state levels, except for the MoO_3 containing catalyst which show a slightly decreasing NO_2 concentration with time at 200 and 225 °C. The step at 225 °C was repeated and the period was increased to 215 min. The NO_2 concentration in this experiment (not shown) continued to decrease with time while, the NO concentration increased and the NO_x concentration was stable. This means that the decreased outlet concentration of NO_2 cannot be related to NO_2 adsorption. One possible suggestion for this deactivation is Pt oxidation formation [37].

The decrease in NO oxidation activity when both NO and SO_2 are present in the feed is also observed in the steady state experiments (compare Figs. 3 and 4). The results from these experiments are also in agreement with the heating ramp experiments, except for the $\text{Pt}/\text{Al}_2\text{O}_3$ catalyst which seems to become more active after performing the heating ramp experiment in presence of both NO and SO_2 . This is seen in the increased NO_2 outlet concentrations at 200 and 225 °C in the steady state experiment with both NO and SO_2 present in the feed which was performed directly after the corresponding ramp experiment. These experiments were repeated (not shown) and the results indicate a further increase in NO oxidation activity for this catalyst. Possibly, the simultaneous exposure of NO and SO_2 at temperatures up to 450 °C has caused sample sintering which means an increase in the Pt particle sizes [36]. The activity enhancement can be related to the increase in the stability against PtO_x formation when the particles become larger [37]. Another suggestion for the NO oxidation activity enhancement is the formation of surface alumina sulphates due to sulphur exposure. Skoglundh et al. [38] have observed an increase in the oxidation activity for a $\text{Pt}/\text{Al}_2\text{O}_3$ catalyst after sulphur exposure due to the formation of sulphated alumina.

The decrease in the NO_2 outlet concentration as a function of time shown by the $\text{MoO}_3/\text{Pt}/\text{Al}_2\text{O}_3$ catalyst at simultaneous NO and SO_2 steady state oxidation experiment is shown by the $\text{WO}_3/\text{Pt}/\text{Al}_2\text{O}_3$, $\text{Pt}/\text{Al}_2\text{O}_3$ catalysts as well. Even for this experiment, the decrease in NO_2 outlet concentration is temperature dependent where, the decrease in NO_2 concentration is only seen at 200 and 225 °C as in the previous case. Further, the decrease in NO_2 formation for the $\text{MoO}_3/\text{Pt}/\text{Al}_2\text{O}_3$ catalyst which was seen previously (in SO_2 free atmosphere) is further enhanced in the presence of SO_2 . Since the presence of SO_2 has altered the stable NO_2 levels for the other catalysts, then the presence of SO_2 may have increased the Pt oxidation.

Enhancing the oxidation resistance for Pt catalysts has previously been studied using XAFS and XANES [39,40]. The authors claim that the addition of electrophilic cations to alumina supported Pt catalysts increases the resistance against Pt oxidation due to the increase in surface acidity. According to these studies, MoO_3 may enhance the Pt oxidation resistance. If the decrease in the NO_2 formation with time delay during the steady state oxidation is a consequence

of Pt oxidation, then our result is in disagreement with the study mentioned above at least for these reaction conditions. On the other hand, the suggested increase in surface acidity in the XAFS and XANES studies were tested by performing propane oxidation experiments [39]. The results from these experiments show an increase in propane oxidation activity for electrophilic cation modified Pt/Al₂O₃ catalysts. In our experiments the presence of NO₂ which is a strong oxidation agent may block the protection effect caused by electrophilic additives at least at some reactions conditions.

From the results and discussion mentioned above, it is clear that MoO₃ and WO₃ have a significant enhancing effect on the NO oxidation also in the presence of SO₂. These two metal oxides are widely used as promoters to enhance the conversion of NO in supported V₂O₅ catalysts for SCR applications [23,24,41,42]. Some researchers relate the enhancement in NO oxidation to the strong redox properties of these metal oxides. This means that parallel to the NO conversion which occur on the active sites, further NO conversion occur on the promoter sites in form of redox cycles which increase the amount of converted NO. The redox activity of these two metal oxides was investigated by performing NO oxidation temperature ramp experiments using MoO₃/Al₂O₃ and WO₃/Al₂O₃ samples. The results (not shown) from those experiments show that neither of the two samples were active for NO oxidation, i.e. the enhancement in NO oxidation for the MoO₃ and WO₃ containing catalysts cannot be related to direct NO oxidation on the promoter sites. On the other hand, NO oxidation can take place on the border site of Mo–Pt and W–Pt or via a spill over process from Pt to Mo and W which means that the presence of these metal oxides may play an important roll in enhancing the NO oxidation activity.

4.2. SO₂ oxidation

As previously, mentioned in the Section 3, the SO₂ adsorption time at room temperature prior to the heating ramp and steady state oxidation experiment varied between the catalysts. This makes the interpretation of the results from the SO₂ heating ramp oxidation experiments complicated. The Pt/Al₂O₃ and Ga₂O₃/Pt/Al₂O₃ catalysts adsorbed much higher amounts of SO₂ during the saturation step. In order to investigate the effect of metal oxide addition on SO₂ oxidation, the SO₂ conversion was calculated both in the absence and presence of NO according to the following formula:

$$SO_{2\text{conv}} = \frac{[SO_2]_{\text{inlet}}(t_f - t_0) - \int_{t_0}^{t_f} [SO_2]_{\text{outlet}} dt}{[SO_2]_{\text{inlet}}(t_f - t_0)}$$

where t_0 and t_f are initial and final time, respectively. We assume that only a minor part of the adsorbed SO₂ will remain on the surface when the temperature ramp is terminated at 450 °C and due to the strong oxidative environment, the difference between the inlet and the outlet SO₂ concentration level is related to SO₂ oxidation to SO₃ and sulphate.

Table 5

Percentage SO₂ converted in the separate SO₂ and simultaneous NO and SO₂ temperature ramp experiments

	SO ₂ conversion (%) with NO in the feed	SO ₂ conversion (%) without NO in the feed
Pt/Al ₂ O ₃	52	34
Ga ₂ O ₃ /Pt/Al ₂ O ₃	49	24
WO ₃ /Pt/Al ₂ O ₃	44	39
V ₂ O ₅ /Pt/Al ₂ O ₃	40	28
MoO ₃ /Pt/Al ₂ O ₃	34	25

The result from this calculation is shown in Table 5, which shows two interesting features: (i) the SO₂ oxidation is promoted in the presence of NO in all catalysts. A possible explanation for this feature is when NO is included in the gas mixture, NO₂ will be formed which is a stronger oxidation agent than oxygen. This means that the environment will be more oxidative, which results in higher SO₂ oxidation capacity. NO₂ is used in the lead chamber process for production of sulphuric acid synthesis just because of the strong oxidation property of NO₂ [43]; (ii) the WO₃ containing catalyst shows high SO₂ oxidation activity in temperature ramp and steady state SO₂ oxidation experiments. In simultaneous NO and SO₂ steady state oxidation, the Pt/Al₂O₃ catalyst shows the highest SO₂ oxidation activity. As it was mentioned previously, this catalyst for some reason became more active after the exposure to SO₂ in oxidative atmosphere at high temperatures (up to 450 °C).

The SO₂ oxidation behaviour in separate SO₂ steady state oxidation differs from the case when NO is included in the gas mixture. In the first mentioned one, all catalysts except the WO₃/Pt/Al₂O₃ catalyst show steady SO₂ levels at all temperatures. The peak in between the steps is due to SO₂ desorption. In the presence of NO, the SO₂ oxidation is promoted and steady SO₂ levels are not reached above 175 °C. The increase in the SO₂ concentrations at each temperature step can possibly be related to the Pt oxidation mentioned previously.

4.3. NO_x storage

From the NO oxidation experiments which were performed prior to the transient lean and rich experiments, two features are observed. First, the presence of BaO leads to lower NO oxidation activity both for Pt/BaO/Al₂O₃ and for Pt/BaO/MoO₃/Al₂O₃. This may be due to dissolution of some amount of BaO during the impregnation with the acidic platinum nitrate solution which may cover some Pt sites or to the formation of more stable Pt-oxides when barium is present [37]. Second, MoO₃ still show some promoting effect on the NO oxidation, but the effect is much lower than for the corresponding catalyst without BaO. The lower promoting effect might be explained by less contact between Pt and MoO₃ in the modified preparation method, or that the interaction between MoO₃ and the basic BaO may reduce the acidity of MoO₃. The reason to include MoO₃ in the

NO_x storage catalyst was the high NO oxidation activity and the relatively low SO₂ oxidation activity for MoO₃/Pt/Al₂O₃ sample compared with the other metal oxide additives. It was thought that an increased NO₂ formation rate would facilitate and improve the NO_x storage and suppressing SO₂ oxidation will end up with lower amount of the thermally stable sulphates which poison the NO_x storage component.

Features which are seen from the transient experiments performed with both the Pt/BaO/Al₂O₃ and the Pt/BaO/MoO₃/Al₂O₃ catalysts and worth to discuss (see Fig. 10) are: (i) the regeneration during the rich conditions is not complete even in the sulphur free cycles (NO_x concentration is not close to zero); (ii) the presence of SO₂ seems to affect the direct reduction where the steady state NO_x level increases directly after the SO₂ exposure has been started; (iii) when SO₂ exposure has begun, the NO_x concentration during the release period increases due to reduction deterioration; (iv) the deterioration of the NO reduction due to sulphur exposure is higher in the Pt/BaO/MoO₃/Al₂O₃ catalyst, where the amount of detected NO_x increase more with time compared to the Pt/BaO/Al₂O₃ catalyst; (v) the concentration of detected NO₂ increases with time which indicate a lower NO_x storage capacity due to formation of barium sulphates.

The amount of stored NO_x in each storage cycle has been calculated according to the calculation method described in [7]. The results from these calculations show a slightly higher storage capacity for Pt/BaO/Al₂O₃, compared with the Pt/BaO/MoO₃/Al₂O₃ sample, both in absence and presence of SO₂, in spite of a higher NO₂ formation for the later catalyst.

From Fig. 11, it is obvious that the deterioration rate of NO_x storage capacity for both catalysts follows the same tendency up to the seventh cycle. Thereafter, the NO_x storage capacity for the Pt/BaO/MoO₃/Al₂O₃ catalyst deteriorates faster than for Pt/BaO/Al₂O₃ catalyst. From Fig. 10, it is clear that the decreased reduction capacity during rich condition for the MoO₃ containing catalyst starts to be significant from the seventh sulphur exposure cycle. Obviously, the faster poisoning in the Pt/BaO/MoO₃/Al₂O₃ catalyst is a consequence of the deteriorated reduction capacity. What that depends on is not clear, but somehow the presence of MoO₃ accelerates the deterioration of the Pt reduction.

The reason that the NO_x storage catalyst with the added promotor was not found to be more sulphur resistant is probably connected to the interaction between sulphur and Pt. We have earlier found that a key component in sulphur deactivation is connected to formation of sulphur species on Pt during rich conditions [21]. This mechanism is obviously not positively influenced by addition of molybdenum oxide.

5. Conclusions

In this work, we have studied the effect of metal oxide additives on enhancing NO oxidation and/or suppressing

SO₂ oxidation in alumina supported Pt catalysts. The main conclusions are summarised below.

Catalysts without NO_x storage material:

- In the absence of SO₂, WO₃/Pt/Al₂O₃ and MoO₃/Pt/Al₂O₃ show the highest NO oxidation promoting.
- In the presence of SO₂, the NO oxidation activity is decreased for all catalysts.
- The decrease in NO oxidation activity due to SO₂ exposure was highest for the Pt/Al₂O₃ and the Ga₂O₃/Pt/Al₂O₃ catalysts followed by WO₃/Pt/Al₂O₃ and V₂O₅/Pt/Al₂O₃ catalysts and finally MoO₃/Pt/Al₂O₃ catalyst.
- The MoO₃/Pt/Al₂O₃ catalyst was the most efficient catalyst in enhancing the NO oxidation while suppressing the SO₂ oxidation.
- For all catalysts, SO₂ oxidation was promoted in the presence of NO in the reaction gas mixture.

NO_x storage catalysts:

- The Pt/BaO/MoO₃/Al₂O₃ catalyst showed a slightly higher NO oxidation activity than the Pt/BaO/Al₂O₃ catalyst.
- The Pt/BaO/Al₂O₃ and Pt/BaO/MoO₃/Al₂O₃ catalysts store almost the same amount of NO_x in the SO₂ free cycles.
- The Pt/BaO/MoO₃/Al₂O₃ catalyst was sulphur poisoned faster than the Pt/BaO/Al₂O₃ catalyst due to reduction in the regeneration capacity in the rich periods where the outlet NO_x concentration during these periods was increased with time.

Acknowledgements

This work has been performed within the Competence Centre for Catalysis, which is financially supported by the Swedish National Energy Agency and the member companies: AB Volvo, Johnson Matthey-CSD, Saab Automobile Powertrain AB, Perstorp AB, AVL-MTC AB, Akzo Nobel Catalysts and The Swedish Space Corporation.

References

- [1] T.P. Barnett, D.W. Pierce, R. Schnur, *Science* 292 (2001) 270–274.
- [2] S. Levitus, J.I. Antonov, J. Wang, T.L. Delworth, K.W. Dixon, A.J. Broccoli, *Science* 292 (2001) 267–270.
- [3] R.M. Heck, R.J. Farrauto, *Catalytic Air Pollution Control*, Van Nostrand Reinhold, New York, 1995, p. 193.
- [4] T. Nakatasuji, R. Yasukawa, K. Tabata, T. Sugaya, K. Ueda, *SAE Technical Paper Series* 980932, 1998.
- [5] E. Fridell, H. Persson, B. Westerberg, L. Olsson, M. Skoglundh, *Catal. Lett.* 66 (2000) 71–74.
- [6] E. Fridell, M. Skoglundh, B. Westerberg, S. Johansson, G. Smedler, *J. Catal.* 183 (1999) 196–209.
- [7] P. Engstrom, A. Amberntsson, M. Skoglundh, E. Fridell, G. Smedler, *Appl. Catal. B: Environ.* 22 (1999) L241–L248.
- [8] H. Mahzoul, J.F. Brilhac, P. Gilot, *Appl. Catal. B: Environ.* 20 (1999) 47–55.

- [9] H. Mahzoul, P. Gilot, J.-F. Brilhac, B.R. Stanmore, *Top. Catal.* 16–17 (2001) 293–298.
- [10] T. Nakatsuji, R. Yasukawa, K. Tabata, K. Ueda, M. Niwa, *Appl. Catal. B: Environ.* 21 (1999) 121–131.
- [11] J.P. Breen, M. Marella, C. Pistarino, J.R.H. Ross, *Catal. Lett.* 3–4 (2002) 123–128.
- [12] N.M. Popova, A.K. Umbetkaliev, K. Dosumov, N.A. Antonova, *React. Kinet. Catal. Lett.* 57 (1996) 255–262.
- [13] E. Fridell, H. Persson, L. Olsson, B. Westerberg, A. Amberntsson, M. Skoglundh, *Top. Catal.* 16–17 (2001) 133–137.
- [14] S. Salasc, M. Skoglundh, E. Fridell, *Appl. Catal. B: Environ.* 36 (2002) 145–160.
- [15] A. Amberntsson, P. Engström, H. Persson, B. Kasemo, *Appl. Catal. B: Environ.* 31 (2001) 27–38.
- [16] A. Amberntsson, M. Skoglundh, M. Jonsson, E. Fridell, *Catal. Today* 73 (2002) 279–286.
- [17] K. Yamazaki, T. Suzuki, N. Takahashi, K. Yokota, M. Sugiura, *Appl. Catal. B: Environ.* 30 (2001) 459–468.
- [18] S.I. Matsumoto, Y. Ikeda, H. Suzuki, M. Ogai, N. Miyoshi, *Appl. Catal. B: Environ.* 25 (2000) 115–124.
- [19] N. Miyoshi, S. Matsumoto, *Sci. Technol. Catal.* 36 (1998) 245–250.
- [20] H. Hirata, I. Hachisuka, Y. Ikeda, S. Tsuji, S.I. Matsumoto, *Top. Catal.* 16–17 (2001) 145–149.
- [21] A. Amberntsson, M. Skoglundh, S. Ljungström, E. Fridell, *J. Catal.* 217 (2003) 245–252.
- [22] H.S. Gandhi, M. Shelef, *Appl. Catal.* 77 (1991) 175–186.
- [23] J.P. Dunn, H.G. Stenger Jr., I.E. Wachs, *Catal. Today* 53 (1999) 543–556.
- [24] J.P. Dunn, H.G. Stenger Jr., I.E. Wachs, *Catal. Today* 51 (1999) 301–318.
- [25] M.D. Amiridis, R.V. Duevel, I.E. Wachs, *Appl. Catal. B: Environ.* 20 (1999) 111–122.
- [26] M.A. Larrubia, G. Busca, *Mater. Chem. Phys.* 72 (2001) 337–346.
- [27] L. Dall’Acqua, I. Nova, L. Lietti, G. Ramis, G. Busca, E. Giamello, *PCCP Phys. Chem. Chem. Phys.* 2 (2000) 4991–4998.
- [28] J. Pasel, V. Speer, C. Albrecht, F. Richter, H. Papp, *Appl. Catal. B: Environ.* 25 (2000) 105–113.
- [29] M. Haneda, Y. Kintaichi, H. Shimada, H. Hamada, *J. Catal.* 192 (2000) 137–148.
- [30] M. Haneda, Y. Kintaichi, H. Hamada, *Appl. Catal. B: Environ.* 31 (2001) 251–261.
- [31] M. Haneda, Y. Kintaichi, H. Hamada, *Catal. Today* 54 (1999) 391–400.
- [32] A.L. Petre, A. Auroux, P. Gelin, M. Caldararu, N.I. Ionescu, *Thermochim. Acta* 379 (2001) 177–185.
- [33] Y.N. Pushkar, A. Sinitsky, O.O. Parenago, A.N. Kharlanov, E.V. Lunina, *Appl. Surf. Sci.* 167 (2000) 69–78.
- [34] M. Skoglundh, H. Johansson, L. Lowendahl, K. Jansson, L. Dahl, B. Hirschauser, *Appl. Catal. B: Environ.* 7 (1996) 299–319.
- [35] P. Lööf, B. Kasemo, S. Andersson, A. Frestad, *J. Catal.* 130 (1991) 181–191.
- [36] A.F. Lee, K. Wilson, R.M. Lambert, C.P. Hubbard, R.G. Hurley, R.W. McCabe, H.S. Gandhi, *J. Catal.* 184 (1999) 491–498.
- [37] L. Olsson, E. Fridell, *J. Catal.* 210 (2002) 340–353.
- [38] M. Skoglundh, A. Ljungqvist, M. Petersson, E. Fridell, N. Cruise, O. Augustsson, E. Jobson, *Appl. Catal. B: Environ.* 30 (2001) 315–328.
- [39] Y. Yazawa, H. Yoshida, T. Hattori, *J. Synchr. Radiat.* 8 (2001) 560–562.
- [40] H. Yoshida, Y. Yazawa, N. Takagi, A. Satsuma, T. Tanaka, S. Yoshida, T. Hattori, *J. Synchr. Radiat.* 6 (1999) 471–473.
- [41] C. Orsenigo, A. Beretta, P. Forzatti, J. Svachula, E. Tronconi, F. Bregani, A. Baldacci, *Catal. Today* 27 (1996) 15–21.
- [42] J.P. Dunn, J. Stenger, G. Harvey, I.E. Wachs, *J. Catal.* 181 (1999) 233–243.
- [43] P. Roebuck, *Chem. Br.* 32 (1996) 38–41.